Cover Page

Mineral Precipitation in the Rotokawa Geothermal Power Station, New Zealand

K.T. WARD[1]
SGGES, University of Auckland, NZ

K.L. BROWN[2]
GEOKEM, Auckland, NZ

J. WEBSTER-BROWN[1]
SGGES, University of Auckland, NZ

Total No of pages = 6

[1]SGGES, University of Auckland, Private Bag 92019 Auckland Mail Centre, Auckland 1142, New Zealand
Ph. +64(09)373-7599   Fax +64(09)3737435

[2]GEOKEM, PO Box 95210, Swanson, Auckland, New Zealand

Proceedings 28th NZ Geothermal Workshop 2006

MINERAL PRECIPITATION IN THE ROTOKAWA GEOTHERMAL POWER STATION, NEW ZEALAND

K.T. WARD[1], K.L BROWN[2] AND J. WEBSTER-BROWN[1]

[1]University of Auckland, New Zealand
[2]GEOKEM, Auckland, New Zealand

SUMMARY – Scaling in production pipelines and heat exchangers in the Rotokawa geothermal power station occurs through changes in physico-chemical properties of the fluids. Reservoir fluids at ~330°C are flashed to 265°C with an accompanying pressure reduction from 70 to 50bar abs. This major pressure reduction causes the precipitation of altaite, hessite, sphalerite and pyrite aggregates in a chalcopyrite matrix. Separated liquids at 220°C enter the brine heat exchanger, and undergo conductive cooling. This causes the deposition of altaite, hessite, chalcopyrite, pyrite, wurtzite, quartz and sodic feldspar. Pyrrhotite and Fe oxide are deposited as corrosion products and well scale from the RK5 two phase production pipeline has also been remobilised and redeposited here. Scaling in the brine + condensate heat exchanger occurs as alternating bands of stibnite and kaolinite, with rare tellurides: coloradoite, telluroantimony, altaite and stutzite. Scaling throughout the power station has been thermodynamically modelled using CHILLER and SOLVEQ. Results suggest that deposition of these minerals can be directly related to changes in temperature, pressure, pH and concentration of H_2S.

1. INTRODUCTION

Scaling in geothermal power plants is a consequence of the production of high temperature geothermal resources. The precipitation of scale in production pipelines causes diminished heat transfer capacity, reducing the efficiency of heat extraction (Gunnarsson and Arnorsson, 2005).

The Rotokawa Geothermal System is located in the Taupo Volcanic Zone, New Zealand, approximately 20km northeast of Taupo. The Rotokawa geothermal power station is a combined cycle Rankine steam turbine/binary plant with a capacity of 33MW. Scaling in the Rotokawa production system occurs as silica scale, with high concentrations of sulfide and telluride minerals (Reyes et al., 2002). Scale is deposited within the two phase production pipelines, in the steam and brine lines, in the heat exchangers, and in the reinjection lines. The depositional mechanisms of scaling are boiling and subsequent phase separation, conductive cooling, mixing and subsequent dilution, and changes in pH and in the redox conditions of the fluids (Reyes et al., 2002).

In this paper, we aim to characterise the mineralogy and geochemistry of scaling, and to determine the fluid mineral equilibria in production pipelines and heat exchangers in the Rotokawa geothermal power station.

2. MINERALOGY AND GEOCHEMISTRY

The mineralogy and geochemistry of scale deposits changes with physico-chemical changes throughout the Rotokawa geothermal power station. Samples were taken from the RK5 two phase production pipeline, the turnaround headers in the brine heat exchanger and the brine + condensate preheater heat exchanger.

The mineralogy and geochemistry of the scale deposits were determined using reflected light microscopy, X-ray diffraction (XRD), X-ray fluorescence (XRF), and scanning electron microscopy (SEM).

2.1 RK5 two phase pipeline

Scale deposits were sampled from the RK5 production well two phase pipeline, from both before and after the pressure reduction from a well head pressure of ~70 to ~50bar abs.

XRD analyses of scale from the RK5 production pipeline upstream of the pressure control valve show a dominantly chalcopyrite ($CuFeS_2$) spectra, with minor altaite (PbTe). Pyrrhotite ($Fe_{1-x}S$), which is likely formed as a corrosion product and detrital smectite [$(Al,Mg)_4Si_8O_{20}(OH)_4X_{0.85}nH_20)$] and calcite ($CaCO_3$) are also present in these samples. An amorphous phase is indicated by a broad hump within the XRD spectra from ~11°2θ to 23°2θ.

Using reflected light microscopy, scale deposits from downstream of the RK5 pressure control valve were identified as bands of amorphous silica in a matrix composed of intergrowths of chalcopyrite, pyrite (FeS_2), sphalerite (ZnS), hessite (Ag_2Te) and altaite. The mineral intergrowths display a unidirectional growth pattern in a series of poorly developed dendrites. These dendrites bifurcate upwards as aggregates of very fine grained subhedral crystals from branches adhered to bands of amorphous silica.

XRD analyses of scale from downstream of the pressure control valve are characterised by chalcopyrite with minor altaite and hessite. Low background XRD spectra suggest there is only a little amorphous phase present.

XRF analyses of scale deposit from downstream of the RK5 pressure control valve give concentrations of Te 4.69 wt%, Ag 7.15 wt% and Au 0.21 wt% as shown in Table 1.

Scanning electron microscopy was used to provide a semiquantitative elemental analysis using an energy dispersive X-ray microanalyser (EDS). EDS analysis of RK5 scale deposits determined the presence of petzite (Ag_3AuTe_2) intergrown within the chalcopyrite aggregates.

The paragenesis of well scale from downstream of the RK5 pressure control valve is evident in backscatter SEM images. These images indicate that altaite and petzite deposited first, followed by hessite, sphalerite/pyrite and finally chalcopyrite (Figure 1A).

Table 1 – Representative XRF analyses (wt %) of RK5 downstream of the pressure control valve, brine heat exchanger level 6 turnaround header (OEC1) and the brine + condensate heat exchanger preheater tube plate (OEC21).

Element	RK5	OEC1	OEC21
O	21.70	41.12	41.51
Al	0.59	1.14	18.44
Si	7.56	31.06	21.00
S	21.50	7.11	4.85
Cl	0.00	0.02	0.25
K	0.23	2.05	0.56
Ca	0.10	0.79	0.75
V	0.00	0.01	0.28
Fe	20.18	6.99	0.86
Cu	12.30	2.30	0.13
Zn	2.02	0.32	0.02
As	0.00	0.00	0.34
Mo	0.00	0.00	0.51
Ag	7.15	1.23	0.08
Sb	0.00	0.00	9.24
Te	4.69	0.93	0.27
Au	0.21	0.04	0.00
Hg	0.00	0.00	0.03
Pb	1.41	0.31	0.02

2.2 Brine heat exchanger

Three samples were taken from the brine heat exchanger, from the level 6 turnaround header, the level 4 turnaround header and the heat exchanger inlet. The mineralogy of scale sample from the inlet consists of a cemented ‘breccia’, where pipeline scale has been remobilised and transported downstream of the initial site of deposition. ‘Breccia’ clasts consist of the well scale aggregates found in RK5 pipelines and chalcopyrite, pyrrhotite, pyrite, quartz (SiO_2), Fe oxide and sodic feldspar $[(Na,Ca)[Al(Si,Al)Si_2O_8)]$.

XRD analyses of scale from the brine heat exchanger inlet are characterised by quartz, sodic feldspars, chalcopyrite, pyrite and pyrrhotite. A hump in the spectra from 15 to 32 degrees 2θ indicates a significant amorphous phase in the sample. XRD analysis of samples from the level 6 turnaround header and the level 4 turnaround header are dominated by chalcopyrite and quartz peaks with associated sodic feldspar, pyrite, and wurtzite (ZnS), and a significant amorphous phase.

Under backscatter SEM the amorphous phase is seen as silica colloids which occur in globular textures, nucleating on Fe-rich pipeline corrosion products. In the interstices of the opaline colloid aggregates, chalcopyrite has deposited with altaite, hessite and pyrrhotite (Figure 1B). Fe-oxide occurs in fibrous concentric textures and is common corrosion product throughout brine heat exchanger.

Pyrrhotite occurs in a colloform texture, as coarse crystals radiating from the finer grained bands, and as lathe like needles intergrown with an Al/Mg silicate within the brine heat exchanger ‘breccia’ (Figure 1C). Subhedral altaite and hessite are deposited within coarse grained pyrrhotite needles indicating earlier paragenesis.

XRF analyses of scale deposits from the brine heat exchanger gives a high silica content of 31.06 wt% (Table 1). There is a marked decrease in the concentration of transition metals such as Cu, Fe and Zn compared to precipitates from the RK5 production pipelines. In the brine heat exchanger, Te concentrations have decreased from 4.69 to 0.93 wt%, and Ag and Au concentrations have also decreased significantly.

2.3 Brine + condensate heat exchanger

Mineral precipitates from the brine + condensate heat exchanger occur as concentric scaling deposited in circular pre-heater pipes, and were also collected as unconsolidated deposits scraped from the preheater tube plate. The mineralogy of the scale is characterised by alternating bands of kaolinite ($Al_2Si_2O_5(OH)_4$) and stibnite (Sb_2S_3) (Figure 1D).

Kaolinite forms by crystallisation of previously precipitated colloidal particles (Figure 1E). Stibnite is deposited in colloform bands and as acicular needles intergrown with kaolinite. Arsenic is found substituting for Sb in stibnite. This is reflected in XRF analyses of the brine + condensate heat exchanger where As constitutes 0.34 wt% of the scale whereas it is notably absent in XRF analyses of RK5 production pipeline scale and analyses of the brine heat exchanger.

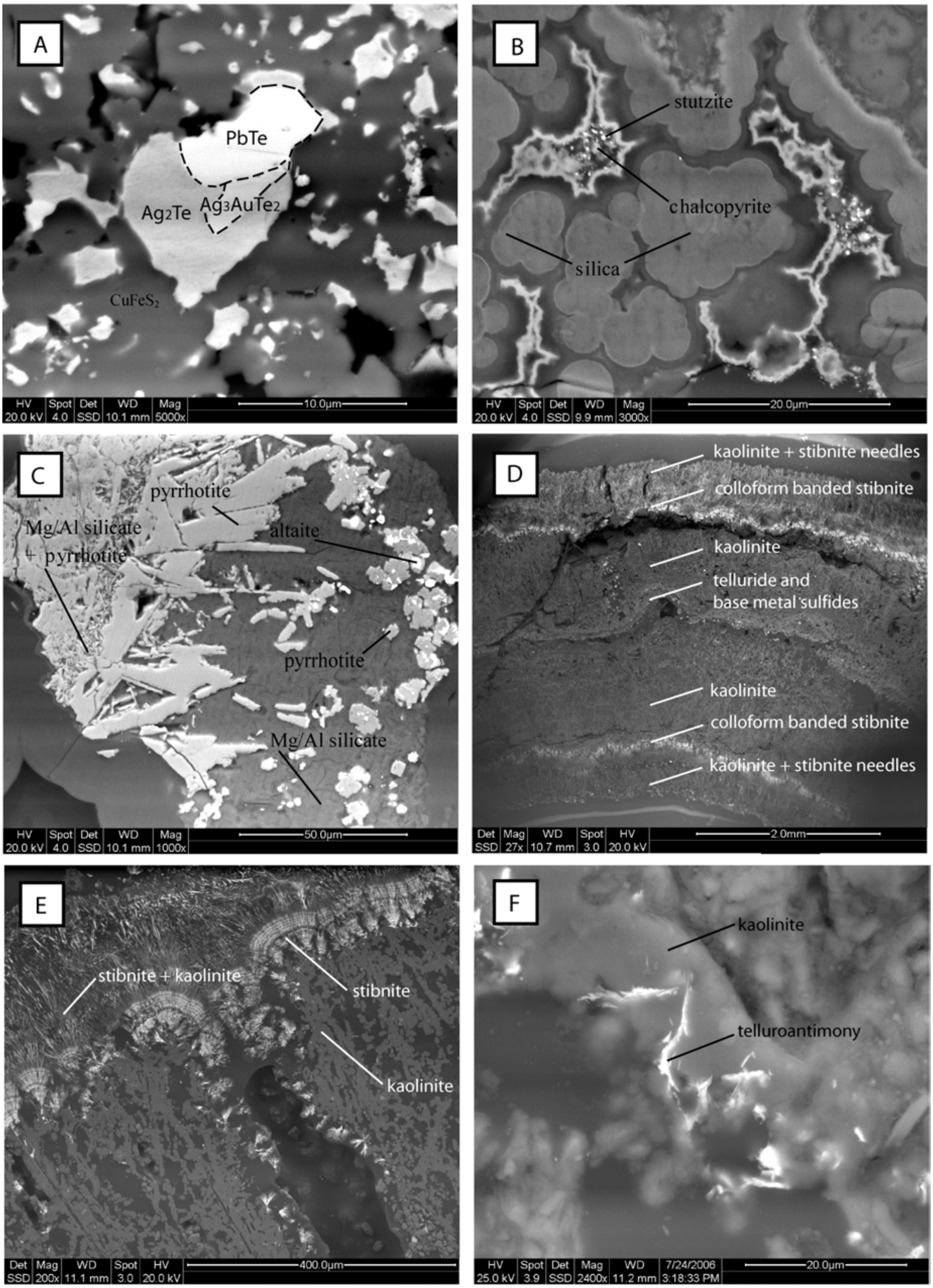

Figure 1 SEM images (A) Scale sample from the RK5 production pipeline, downstream of the pressure control valve showing paragenesis whereby petzite precipitates first followed by altaite, hessite, and finally chalcopyrite (B) Fe-rich silica colloids with chalcopyrite and stutzite between globular opaline aggregates (C) 'Clast' from the brine heat exchanger breccia deposit showing pyrrhotite as lathes, as fine grains intergrown with an Al/Mg silicate, and encompassing an altaite grain (D) Concentric banding showing alternating kaolinite and stibnite in the brine + condensate heat exchanger (E) Kaolinite deposits as colloids and becomes crystalline with equilibration, while stibnite occurs in both colloform bands and as acicular needles within kaolinite in the brine + condensate heat exchanger (F) telluroantimony ribbons and kaolinite in the brine + condensate heat exchanger.

Telluride minerals are deposited in thin bands following periods of kaolinite precipitation. These tellurides (coloradoite (HgTe), telluroantimony (Sb_2Te_3), stutzite ($Ag_{5-x}Te_3$) and altaite) are deposited with chalcopyrite, pyrite and sphalerite. Gold substitutes for up to 15wt% Ag in silver telluride minerals. Telluroantimony occurs in ribbon-like textures (Figure 1F) and coloradoite occurs as anhedral grains within a kaolinite matrix. Pyrite dominantly occurs with a pyritohedra habit. Gold and silver tellurides, altaite and sphalerite occur in aggregates with subhedral to euhedral chalcopyrite.

XRD analyses of samples from the brine + condensate heat exchanger were dominated by the presence of stibnite and kaolinite. The unconsolidated sample scraped from the pre-heater tube plate had more stibnite than kaolinite, whereas the tube-like samples had more kaolinite than stibnite. Scaling in the pre-heater tube plate occurred with magnetite and quartz. Scaling in the return end of the pre-heater channel head occurred with pyrite and quartz. The presence of an amorphous phase is suggested by a diffuse peak in the spectra from 20 to 30 degrees 2θ.

Three brine + condensate heat exchanger samples were analysed using XRF (Table 1). The unconsolidated sample had Sb concentrations up to 25wt % while the tube-like samples had Sb concentrations of up to 9.24 wt%.

3. FLUID MINERAL EQUILIBRIA

The fluid mineral equilibria of the system are determined using the thermodynamic modelling programs, WATCH (Bjarnason, 2004), SOLVEQ (Spycher and Reed, 1998) and CHILLER (Reed and Spycher, 2000). WATCH, and the input file WAIN, were used to combine the liquid and steam phase chemical analyses to provide an estimate of the chemical composition of the reservoir fluids. SOLVEQ and CHILLER were used to calculate the fluid mineral equilibria, modelled at major physico-chemical changes within the system. SOLVEQ and CHILLER use the thermodynamic data base SOLTHERM.

Thermodynamic predictions were made for reservoir fluid flashed to 265°C and ~50 bar abs. (absolute), 226°C and ~25 bar abs., and the separated fluid at 220°C and ~23 bar abs. The fractionated separator fluid was then used as an input to the heat exchangers. A spreadsheet was used in the brine + condensate heat exchanger to combine the two fluids.

The initial reservoir fluid was assumed to have the liquid and vapour phase components outlined in Table 2. The deep fluid component was then derived for a temperature of 330°C at a corresponding pressure of 128 bar abs. using WATCH.

Table 2 - Reservoir fluid chemistry (pers comm.)

Water Sample	**(mg/kg)**
CO_2	69.2
H_2S	16.6
NH_3	5.2
B	18.9
SiO_2	948
Na	402
K	116
Ca	0.71
F	3.6
Cl	747
SO_4	4.7
Al	1.02
Ag	2.4
As	1.4
Au	0.023
Cu	0.003
Fe	0.02
Pb	0.81
Sb	0.227
Te	2.96
Zn	0.88
Steam Sample	**mmoles/100moles of steam**
CO_2	726
H_2S	40
H_2	3.9
N_2	9.1
CH_4	19.8
NH_3	2.6

3.1 Reservoir Fluid Flashed to 265°C

Reservoir fluids are initially flashed from 330°C (pH = 5.74) to 265°C (pH = 6.14) with a well head pressure of ~50 bar abs. CHILLER was used to determine which minerals were thermodynamically predicted to precipitate on flashing.

At the temperature reduction to 325°C, altaite, hessite, calaverite ($AuTe_2$), chalcopyrite, sphalerite and tellurium (Te) are thermodynamically predicted to precipitate. On further pressure and temperature reduction to 320°C daphnite [$(Fe,Mg)_5Al(Si,Al)_4O_{10}(OH)_8$] is predicted to precipitate. Muscovite ($KAl_2(AlSi_3O_{10})(F,OH)_2$), pyrite and pyrophyllite (Al,Si_2O_5OH) are also predicted to deposit from the solution on flashing to 265°C. This provides a thermodynamic prediction which is consistent with the paragenetic sequence found downstream of the RK5 pressure control valve.

3.2 Fluid Flashed to 220°C

The fluid is flashed from 265°C to 226°C and the temperature is further reduced to ~220°C (23bar abs.) by the time it reaches the separator. Sphalerite, microcline ($KAlSi_3O_8$) and daphnite are thermodynamically predicted to precipitate on flashing from 265°C to 245°C, with altaite depositing from 245°C to 220°C, followed by pyrite and heulandite ($Ca,Na_{2-3}Al_3(Al,Si)_2Si_{13}O_{36}H_2O_{12}$) at 220°C. This fractionated fluid at 220°C provides an input for the heat exchanger brines.

3.3 Brine Heat Exchanger – Conductive Cooling

From the separator, brine is transported to the brine heat exchanger, where the fluid is conductively cooled from 220°C at a pH of 6.21, to between 170°C (pH = 5.99) and 150°C (pH = 5.89). Thermodynamic predictions were made of mineral precipitation through the conductive cooling depositional mechanism using CHILLER. Altaite, galena (PbS), quartz and sphalerite were predicted to precipitate at 220°C, with pyrite precipitating at 205°C. At 195°C, hessite replaces altaite, with this assemblage predicted to precipitate on the further temperature decrease through to 150°C.

3.4 Brine + Condensate Heat Exchanger – Conductive Cooling

In the brine + condensate heat exchanger, fluids are conductively cooled to between 160 and 115°C. Here, the fluids undergo further physical and chemical changes on addition of variable amounts of steam condensate to the brine in the pre-heater. This fluctuating ratio changes the pH, temperature and concentration of H_2S in the solution, and is taken into consideration using the thermodynamic models.

The regular operating ratio of brine to condensate in the heat exchanger averages around 60-65% brine. The fluid enters the preheater at around 215°C, decreasing to around 120°C, although rarely, outflow temperatures are as low as 100°C. With a brine to condensate ratio of 60% the fluid enters the heat exchanger at a pH of 5.62. Dissociation reactions cause the pH to increase to 5.67, before decreasing again to 5.5 at 100°C. Under these conditions, kaolinite is thermodynamically predicted to precipitate using the SOLVEQ modelling program by conductive cooling of the fluid to 165°C at a pH of 5.67.

Thermodynamic modelling predicts deposition of stibnite with decreasing temperature and pH. Where the $Sb(OH)_3(aq)$ species dominates, stibnite deposition occurs with an increase in H_2S (Zotov et al., 2003). Where thio complex species dominate, however, deposition occurs with a decrease in H_2S concentration (Zotov et al., 2003). This is seen in the OEC21 heat exchanger where at temperatures between 220 and 160°C the hydroxyl species dominates. Here, the precipitation of stibnite is more likely to occur with a brine condensate ratio of 40:60. However, at temperatures below 160°C where the bisulfide antimony species $HSb_2S_4^-$ dominates, precipitation is thermodynamically more likely to precipitate at brine to condensate ratio of 60:40. However, the thermodynamic models suggest that temperature is the dominating factor controlling the precipitation of stibnite in the brine + condensate heat exchanger. Stibnite precipitation is predicted to occur in the heat exchanger on conductive cooling of the fluids to ~130°C.

The lack of thermodynamic data for tellurides has been a limitation in the prediction of precipitation in the heat exchanger. However, altaite is thermodynamically predicted to precipitate within the heat exchanger at a brine to condensate ratio of 80% on conductive cooling of the fluid from 202°C. Chalcopyrite and hessite are not thermodynamically predicted to precipitate within this heat exchanger.

4. CONCLUSIONS

The results of thermodynamic modelling in the Rotokawa geothermal power station are consistent with the mineralogical observations in the scale deposits.

4.1 RK5 two phase pipeline

Reservoir fluids at ~330°C and a corresponding fluid pressure of ~128 bar abs. rise and undergo isenthalpic boiling. At the pressure control valve, reservoir fluids are flashed to ~265°C and ~50 bar abs. When this major temperature and pressure reduction occurs, altaite, hessite, sphalerite and pyrite are deposited as aggregates with a matrix of chalcopyrite.

4.2 Brine heat exchanger

These fluids are flashed again to around 226°C, and are cooled to 220°C by the time they reach the separator. Separated brine enters the brine exchanger where it is conductively cooled to between 170 and 150°C. Altaite, galena, quartz, sphalerite and pyrite are deposited on the initial cooling of the fluids. Hessite requires further conductive cooling to ~195°C, where altaite is no longer in equilibrium with the fluids.

4.3 Brine + condensate heat exchanger

The brine + condensate preheater was cleaned using caustic soda in November 2005, and again with a high water pressure clean in April 2006. Over this period, approximately 4mm of kaolinite/stibnite scale was deposited within the preheater tube. The results of thermodynamic modelling were compared to the physico-chemical changes which occurred in the preheater during the period between the caustic and high pressure cleans.

It was found that mineral precipitation in the heat exchanger is a function of the brine to condensate ratio. This ratio causes changes in temperature, pH, and in the concentration of H_2S in solution, controlling solubility within the heat exchanger. Kaolinite deposits at the regular working conditions of the heat exchanger (~ 60% brine). Deposition requires a pH of 5.6 and a temperature of ≤ 165°C. Deposition of stibnite in the heat exchanger is believed to have occurred where temperature decreased to below 130°C.

Altaite and chalcopyrite were deposited alongside the rare tellurides in the heat exchanger. Due to the lack of thermodynamic data for these minerals, altaite and chalcopyrite are used as a proxy for their mineralisation. Altaite is most likely to precipitate where the brine to condensate ratio is 80:20. Although chalcopyrite is not thermodynamically predicted to precipitate in the brine + condensate heat exchanger, it comes closest to precipitation, on conductive cooling of the mixed fluid with a brine to condensate ratio of 80:20. The deposition of coloradoite, telluroantimony, altaite and the gold/silver tellurides is therefore believed to occur in response to an increase in the brine to condensate ratio to 80:20.

5. ACKNOWLEDGMENTS

We thank Mighty River Power for the access to the power station and thank staff for cooperation and assistance. Thanks to Keith Litchi for samples and photos, to Jeff Mauk for advice on reflected light microscopy, and to Nathaniel Wilson for advice on stibnite deposition in the brine + condensate heat exchanger. Mighty River Power and the New Zealand Tertiary Education Commission provided the funding for this project.

6. REFERENCES

Bjarnason, J., 2004, WATCH, in Group, I.W.C., ed.: Orkustofnun.

Gunnarsson, I., and Arnorsson, s., 2005, Impact of silica scaling on the efficiency of heat extraction from high temperature geothermal fluids: Geothermics, v. 34, p. 320-329.

Reed, M., and Spycher, N., 2000, Users Guide for CHILLER: A Program for Computing Water Rock Reactions, Boiling, Mixing and Other Reaction Processes in Aqueous Mineral Gas Systems and Minplot Guide: Eugene.

Reyes, A., Trompetter, W., Britten, K., and Searle, J., 2002, Mineral deposits in the Rotokawa geothermal pipelines, New Zealand: Journal of Volcanology and Geothermal Research, v. 119, p. 215-239.

Spycher, N., and Reed, M., 1998, SOLVEQ: A Computer Program for Computing Aqueous Mineral Gas Equilibria: Revised Preliminary edition Eugene.

Zotov, A., Shikina, N., and Akinfiev, N., 2003, Thermodynamic properties of the Sb(III) hydroxide complex Sb(OH)3(aq) at hydrothermal conditions: Geochimica et Cosmochimica Acta, v. 67, p. 1821-1836.